ASME/JSME Thermal Engineering Conference: Volume 2
ASME 1995

A MOLECULAR DYNAMICS SIMULATION OF A LIQUID DROPLET ON A SOLID SURFACE

Sohei Matsumoto[1], Shigeo Maruyama and Hideki Saruwatari
Department of Mechanical Engineering
The University of Tokyo
Bunkyo-ku, Tokyo
Japan

ABSTRACT

A liquid droplet placed on a solid surface was simulated by the molecular dynamics method to study the microscopic aspects of the solid-liquid contact. Four hundred argon molecules were employed to create a liquid droplet and the surrounding vapor. The solid surface was represented by a single layer of fcc lattice made of fixed Lennard-Jones particles. The energy scale ε_{sl} of the inter-molecular potential between solid and liquid molecules and the system temperature T were changed to reproduce various shapes of droplets. Two-dimensional density and potential energy distributions obtained for various values of the solid-liquid potential parameter ε_{sl} showed a strong dependency of the droplet shape on the magnitude of the interaction of solid and liquid molecules. The density distributions revealed the layered structure of the liquid molecules near the solid surface. However, the dependency of the estimated contact angle on various parameters was not far from the simple energy balance concept of a macroscopic liquid drop.

NOMENCLATURE

h	= height measured from the surface
N_v	= the number of vapor molecules
R	= radius of droplet
r	= radius measured from the center of droplet
T	= temperature
ε	= energy scale of L-J potential
ε^*	= non-dimensional energy scale, $\varepsilon_{sl}/\varepsilon_l$
$\phi(r)$	= potential function
γ	= surface free energy
θ	= contact angle
σ	= length scale of L-J potential

Subscripts

c	= center of droplet
g	= vapor
l	= liquid
s	= solid

INTRODUCTION

The microscopic mechanism of solid-liquid contact is the fundamental issue to understand the phase change phenomena such as the dropwise condensation on a solid surface and the collapse of film boiling leading to the transition boiling. The physical mechanism of solid-liquid contact is, however, not sufficiently understood. Recently, the simulation of the liquid-vapor interface by the molecular dynamics method has become the powerful technique to get physical insights into the interface properties such as surface tension (Maruyama et al., 1994a; Maruyama et al. 1994b; Matsumoto, 1994; Nijmeijer et al., 1992) and condensation coefficient (Matsumoto and Kataoka, 1992). However, little is known about the microscopic dynamics of the solid-liquid contact where three phases: solid, liquid and vapor coexist.

In this paper, we report our attempts to investigate the microscopic mechanism of solid-liquid contact using molecular dynamics simulations of a tiny liquid droplet placed on a solid surface. For the purpose of obtaining a basic knowledge on the phenomena, we have chosen a rather simple system as the calculation model. The system included two groups of molecules: one was for the liquid droplet and its vapor, the other for the solid surface. Only the molecules of the former group were computed; the molecules for the solid were fixed at grid points. Although our model of the solid surface does not seem realistic, our preliminary simulations with several types of surface models have suggested that the complicity of the solid model was not so important as far as the results discussed in this

[1]Current Address: Mechanical Engineering Laboratory, Agency of Industrial Science and Technology /MITI, Tsukuba, Ibaraki, Japan

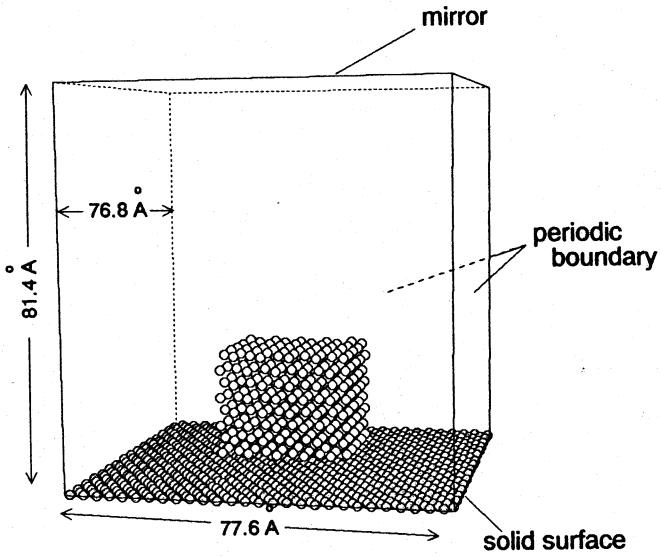

FIG. 1 CALCULATION REGION AND THE INITIAL CONFIGURATION OF MOLECULES

paper were concerned. We assumed Lennard-Jones potential functions for both liquid-liquid and solid-liquid interactions. The parameter ε_{sl} for the solid-liquid potential function can be regarded as a measure of the affinity between the solid and the liquid. Thus we have paid the special attention on the effect of the solid-liquid affinity on the states of contact, including the structure of the interface region and the shape of the droplet as a whole, by applying various values for this parameter. The effect of the temperature was also speculated from simulations of two different system temperatures.

DESCRIPTION OF SIMULATIONS

The molecular dynamics simulation was designed to achieve a stable equilibrium state of liquid droplet and its vapor on a solid surface under the *NVE* ensemble, i.e. the number of molecules, volume and total energy of the system were kept constant. Fig. 1 illustrates the calculation region and the initial configuration of molecules. The region had a mirror boundary (or a hard wall boundary) for the top wall and periodic boundaries for the four side walls. The solid surface located at the bottom of the calculation region was represented by one layer of molecules on a (111) plane of the fcc lattice structure. The lattice constant 2.77 Å was employed after that of the platinum. We ignored the motion of these particles and the influence from the molecules beneath the one layer. It is noteworthy that this stationary molecules was an adiabatic boundary since there was no energy transfer through the surface.

The liquid drop and the vapor were formed of argon molecules. The interactions between molecules were expressed by the following Lennard-Jones potential function.

$$\phi(r) = 4\varepsilon\left\{(\sigma/r)^{12} - (\sigma/r)^{6}\right\} \qquad (1)$$

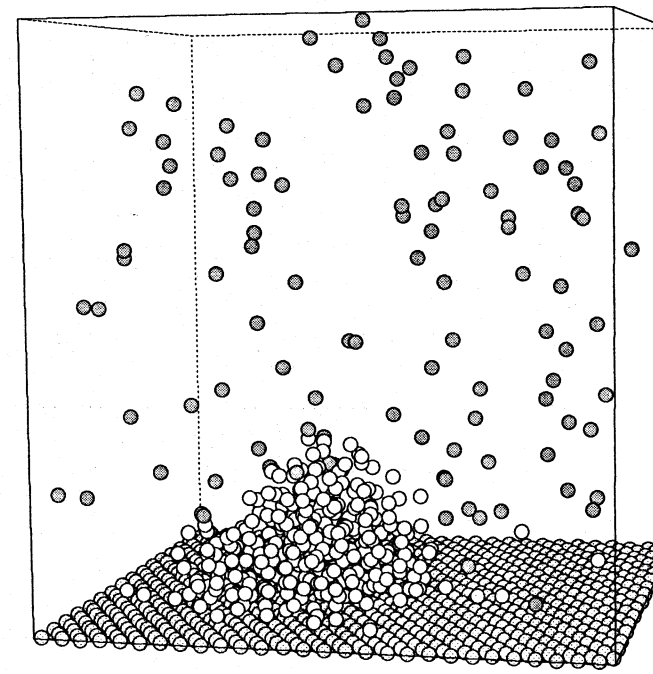

FIG. 2 A SNAPSHOT OF A GENERATED DROPLET ON THE SOLID SURFACE (E2: T = 95K, ε^* = 0.344)

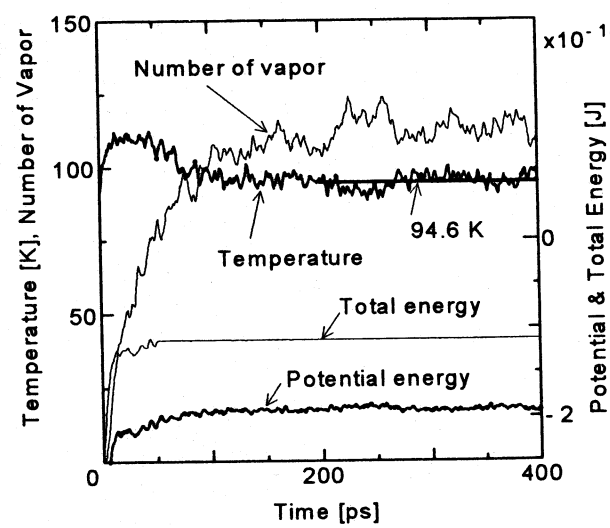

FIG. 3 NUMERICAL EVAPORATION AND EQUILIBRIUM OF A DROPLET (E2: T = 95K, ε^* = 0.344)

Values of parameters were σ_l = 3.4 Å, $\varepsilon_l = 1.67 \times 10^{-21}$ J for liquid-liquid interaction. As for the solid-liquid interaction, σ_{sl} was determined by taking average of the lattice constant of the solid and σ_l. On the other hand, ε_{sl} was implicitly specified through a non-dimensional parameter $\varepsilon^* = \varepsilon_{sl} / \varepsilon_l$ as one of the calculation conditions.

The system contained four hundred argon molecules which

TABLE 1 CONDITION AND CONTACT ANGLE

Label	ε^*	T [K]	N_v	R [Å]	h_c [Å]	θ
E1	0.240	95.1	134	15.0	10.66	135.4°
E2	0.344	94.6	113	17.0	4.62	105.8°
E3	0.449	94.4	94	20.0	-1.02	87.0°
E4	0.554	93.9	94	30.6	-17.46	55.2°
E2C	0.344	84.2	46	18.1	5.66	108.2°
E4C	0.554	83.2	38	30.1	-14.62	60.9°

were arranged in a piece of fcc crystal as displayed in Fig. 1 at the beginning of the calculation. They were located so that the bottom of the crystal aligned at the plane of the minimum of the potential field arising from the solid surface. It was suggested again from our preliminary calculations, the initial configuration of liquid molecules did not make any major differences in the final equilibrium state of the droplet. We have demonstrated that much taller or shorter arrangements of initial argon molecules resulted the same final shape.

For argon molecules the equation of motion was numerically integrated utilizing the Verlet algorithm (Allen and Tildesley, 1987) with a time step of 0.01 ps. Typically first 50 ps of the calculation was spent for the temperature compliance and molecules were velocity-controlled. This was necessary because the kinetic energy in the system was consumed as the latent heat required in the collapse of lattice structure and the vaporization. Then an idling period for the equilibration followed taking typically 100 ps without any operation on the velocity. The establishment of the equilibrium condition was judged through monitoring the temperature, potential energy, and the number of vapor as discussed in more detail in the next section. After the achievement of the equilibrium state the statistics were accumulated every 0.5 ps.

RESULTS AND DISCUSSIONS

Simulations were performed under two temperature ranges extensively changing the parameter $\varepsilon^* = \varepsilon_{sl}/\varepsilon$. Fig. 2 shows a snapshot of a resulting droplet adherent to the solid surface. We observed a round-shaped droplet apart from the surface for small values of ε^* and a liquid layer completely spread out on the surface for large values. A droplet like in Fig. 2 was generated only when the value of ε^* fell in a certain range. All the six cases summarized in Table 1 were found to be in this range.

In Fig. 3 the temperature, potential energy, and total energy of the system as well as the number of vapor molecules are plotted versus time for the case E2. An argon molecule was distinguished as the vapor molecule when the potential perceived by it was larger than a threshold value of -2.5×10^{-21} J (see Fig. 5 and Fig. 7). An example of this distinction of vapor molecules is demonstrated in Fig. 2, where vapor molecules are shown in dark symbols compared with the liquid molecules in open symbols. Except for a few ambiguous molecules near the liquid-vapor and solid-vapor interfaces, the distinction is satisfactory. Sometimes the dimer and the trimer in the vapor area were detected as 'liquid' molecules. Even though more

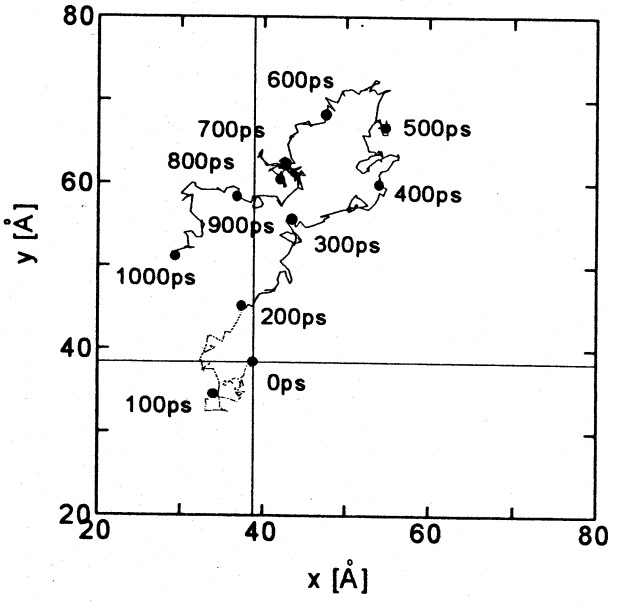

FIG. 4 TRAVEL OF THE DROPLET FOR E2

sophisticated criterion of the molecule state is possible by counting the number of neighbor molecules (Maruyama et al., 1994a; Matsumoto, 1994), we have used this simple technique in this study. The temperature, potential energy and the number of vapor molecules were monitored to detect whether the system arrived at an equilibrium state. In this case in Fig. 3, we decided the system had reached the equilibrium point in the first 200 ps and used the following 200 ps for the analysis.

One thing particularly interesting which we noticed from the observation was that the center of mass of the droplet did not stay still at its initial position; instead, it traveled around randomly over the solid surface even in the equilibrium state. The motion is described in Fig. 4 as the path of the center of mass in the x-y plain; parallel to the solid surface. Solid symbols are time marks. Notice that we have decided that the equilibrium was achieved at 200 ps in Fig. 3. This drifting motion of the droplet would be accounted for the spatial unbalance of the interaction forces between solid and liquid molecules at their interface. For this drifting motion, it was necessary to relocate the coordinate system according to the instantaneous center of mass of the droplet to derive its averaged shapes in order to compare the results more clearly.

We calculated two-dimensional density and potential energy distributions for each case listed in Table 1 by taking a cylindrical coordinate with the axis of symmetry which was normal to the solid surface at the center of mass of the droplet. Fig. 5 shows a series of number density (left) and potential energy (right) distributions for cases with the temperature of about 95 K and the parameter ε^* increasing from top to bottom. The horizontal and vertical axis of each contour mean the radius from the center of mass and the height measured from the surface, respectively. From these contours we could say that the shape of each droplet is similar to a truncated sphere.

(A) E1

(B) E2

(C) E3

(D) E4

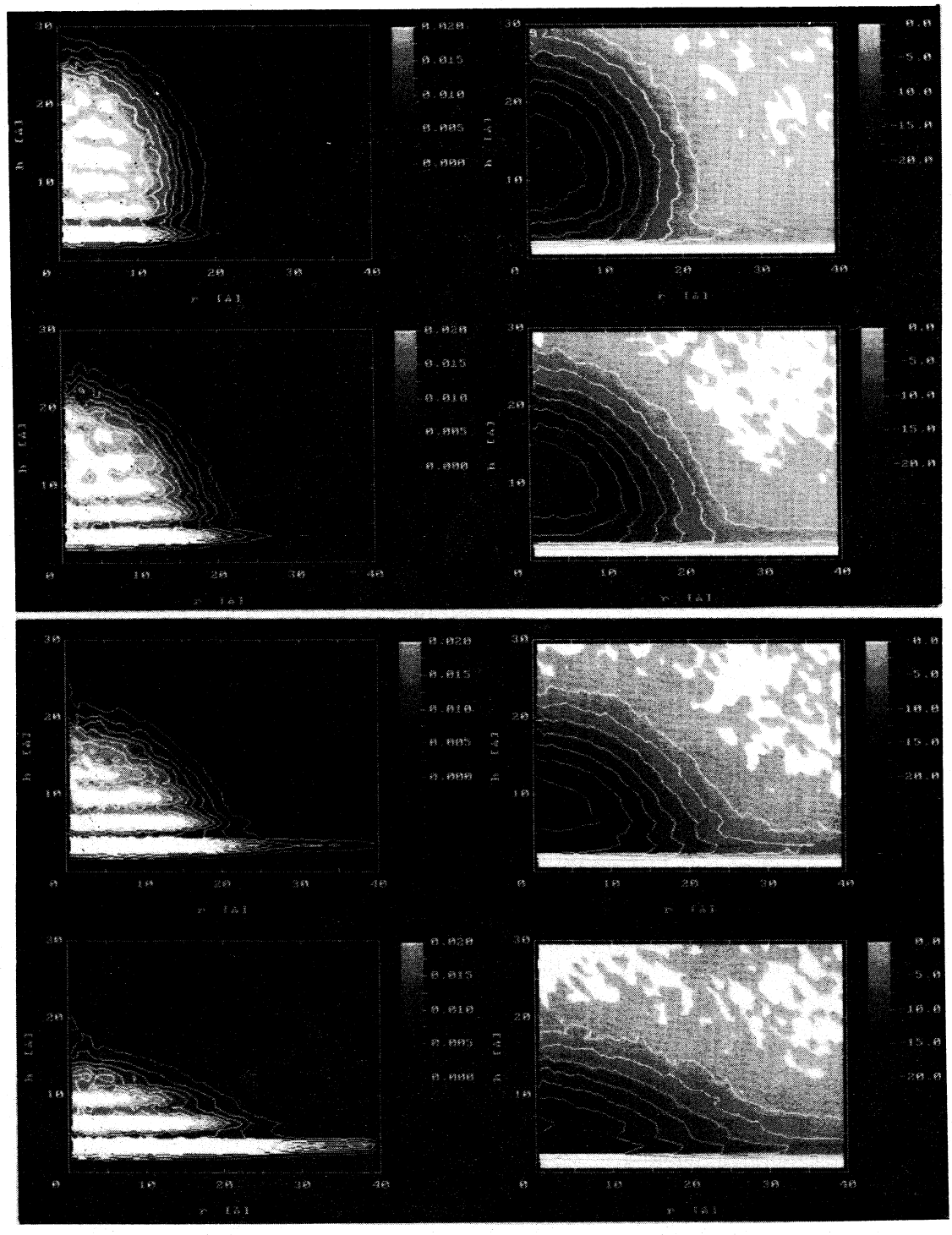

FIG. 5 (A-D) DENSITY (LEFT) AND POTENTIAL (RIGHT) DISTRIBUTIONS. SPACING OF CONTOUR LINES IS 0.0025$Å^{-3}$ FOR DENSITY AND 2.5×10^{-21} J FOR POTENTIAL ENERGY

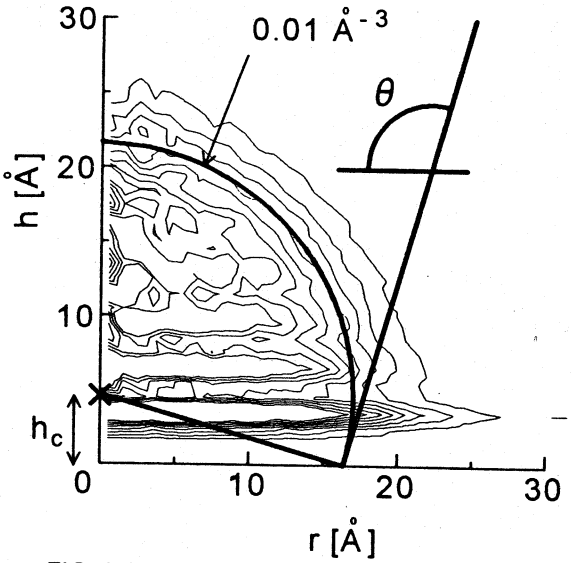

FIG. 6 DEFINITION OF CONTACT ANGLE

The most prominent feature found in the density distribution was the layered structure parallel to the solid surface. The layer next to the surface was particularly significant covering a fairly wide area on the solid compared to the size of the droplet. The layered structure was also observed near the core of the droplet where the local number density was comparable to the saturated bulk liquid density, while the influence of the solid surface was invisible in the liquid-vapor interface region. In contrast, these characteristics were not emphasized in the potential energy distributions except for the first layer. The effect of the solid-liquid affinity parameter ε^* is quite obvious from the comparison of four cases in Fig. 5. The spherical part of the droplet became flat and the first layered structure grew wider as ε^* is increased. On the other hand, in potential energy distributions simply the gradual change of the shape with ε^* was observed.

We made an attempt to evaluate the 'contact angle' for the sake of looking at the difference in the shape of droplets more quantitatively. Because of the arbitrariness in the determination of liquid-vapor interface and the irregularity of contour lines near the three-phase interface, it is difficult to define such a macroscopic property as the contact angle without ambiguity. In our definition of the contact angle, as illustrated in Fig. 6 (the density distribution, E2), we chose the contour line indicating about half value of the bulk number density: 0.01 $Å^{-3}$ and fit a circle. Here, the least squares fitting method was employed to determine the height of the center of the circle h_c and the radius of the circle R. The contact angle θ can be calculated as $\cos\theta = -h_c / R$. These results are summarized in Table 1. The estimation of the contact angle was insensitive to the choice of the contour line for the fitting. And, the same technique applied to the potential distribution resulted the almost same value of the contact angle.

Fig. 7 contains density and potential energy distributions for

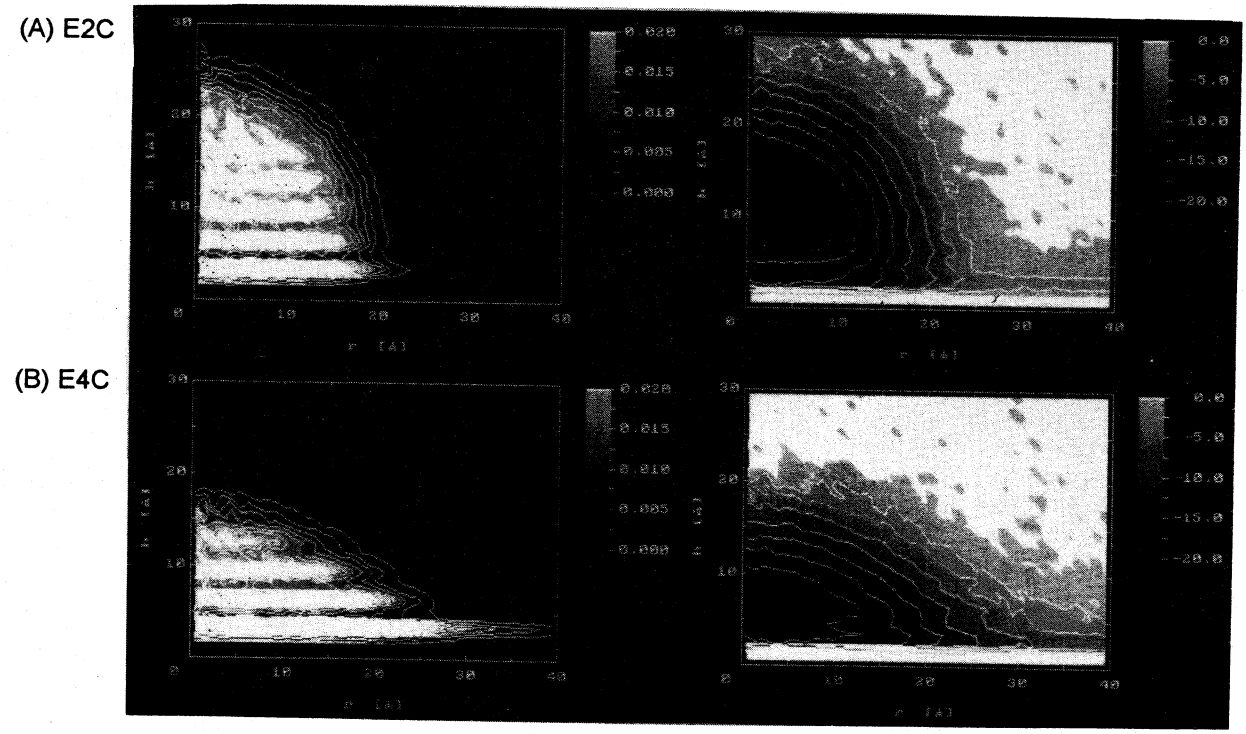

FIG. 7 (A,B) DENSITY (LEFT) AND POTENTIAL (RIGHT) DISTRIBUTIONS FOR LOWER TEMPERATURE, 85K. SPACING OF CONTOUR LINES IS 0.0025 $Å^{-3}$ FOR DENSITY AND 2.5×10^{-21} J FOR POTENTIAL ENERGY

two cases with lower temperature about 85K, in the same way as in Fig. 5. The most obvious effect of the temperature on the shape is seen in the sharpness (or thickness) of the liquid-vapor interface [compare Fig. 5(B) with 7(A), or Fig. 5(D) with 7(B)]. As we have reported previously (Maruyama et al., 1994a; Maruyama et al., 1994b), the density profile and the potential profile are sharper (contour lines are more concentrated) in the lower temperature case.

The evaluated contact angles listed in Table 1 show a slightly larger angle for the low temperature cases. It can be said that the effect of decreasing temperature is similar to the effect of decreasing ε^*, even though the effect of temperature is much weaker. This trend agrees with the macroscopic observation by Shoji and Zhang (1994) that the contact angle decreased with the increase of the system temperature.

Above discussions about the effects of the affinity and temperature seem to lead us to the conclusion that the principal mechanism to determine the droplet shape is a surface energy balance similar to the macroscopic view of the contact angle, in spite of the layered structure in the core region of the droplet which implies quite different properties from the ordinary continuum fluid. The dependency of $\cos\theta$ on ε^* is plotted in Fig. 8. As is clear from the figure, the linear dependency exists between these values. Here, the macroscopic contact angle can be explained by the well known Young's equation,

$$\cos\theta = \left(\gamma_{sg} - \gamma_{sl}\right)/\gamma_{lg} \qquad (2)$$

where γ_{sg}, γ_{sl}, and γ_{lg} are surface free energies (or surface tensions) of solid-vapor, solid-liquid, and liquid-vapor interfaces, respectively. If we simply assume that γ_{sl}/γ_{lg} is proportional ε^* ($=\varepsilon_{sl}/\varepsilon_l$), the macroscopic energy balance (Young's equation) can explain the linear dependency. Then, we can speculate that the simple energy balance concept is actually the governing mechanism of the droplet formation even for the microscopic case.

On the other hand, since $\cos\theta$ is simply $-h_c/R$, which can be regarded as the amount of the submerged deepness of a hypothetical spherical droplet into the surface. Fig. 8 can be interpreted to show that this deepness is proportional to the affinity of the solid and liquid molecules.

CONCLUSION

A liquid droplet adherent to a solid surface was generated by the molecular dynamics simulation. The affinity between solid and liquid molecules was the primary factor to determine the shape of the droplet. The layered structure in the center region of the droplet near the solid surface was observed in the two-dimensional number density distribution; one next to the surface was especially distinguishable making a liquid trail spreading out on the solid. Although these features are the special characteristics of the microscopic droplet, it is suggested that the contact angle can be explained by the surface energy balance

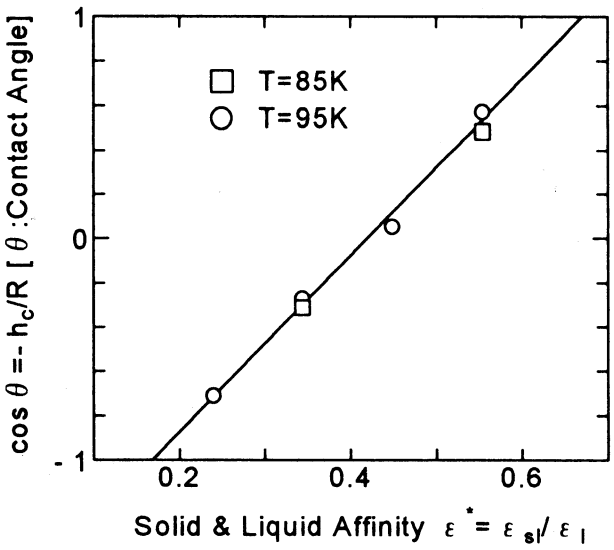

FIG. 8 DEPENDENCY OF THE CONTACT ANGLE ON THE SOLID-LIQUID AFFINITY ε^*.

which is basically equivalent to the macroscopic mechanism.

REFERENCES

Allen, M. P. and Tildesley, D. J., 1987, *Computer Simulation of Liquids*, Oxford University Press, Oxford.

Maruyama, S., Matsumoto, S. and Ogita, A., 1994a, "Surface Phenomena of Molecular Clusters by Molecular Dynamics Method," *Thermal Science and Engineering*, Vol. 2, pp. 77-84.

Maruyama, S., Matsumoto, S., Shoji, M. and Ogita, A., 1994b, "A Molecular Dynamics Study of Interface Phenomena of a Liquid Droplet," *Proceedings 10th International Heat Transfer Conference*, G. F. Hewitt ed., IChemE, Rugby, Vol. 2, pp. 409-414.

Matsumoto, M. and Kataoka, Y., 1992, "Dynamics Processes at a Liquid Surface of Methanol," *Physics Review Letters*, Vol. 69, pp. 3782-3784.

Matsumoto, S., 1994, "Surface Behaviors of a Liquid Droplet by Molecular Dynamics Method," *Transactions of JSME, Series B*, submitted.

Nijmeijer, M. J. P., Bruin, C., van Woerkom, A. B., Bakker, A. F. and van Leeuwen, J. M. J., 1992, "Molecular Dynamics of the Surface Tension of a Drop," *Journal of Chemical Physics*, Vol. 96, pp. 565-576.

Shoji, M. and Zhang, X. Y., 1994, "Study of Contact Angle Hysteresis (In Relation to Boiling Surface Wettability)," *JSME International Journal, Series B*, Vol. 37, pp. 560-567.